Biosensors and Bioelectronics 26 (2011) 3482–3487

Contents lists available at ScienceDirect

Biosensors and Bioelectronics

journal homepage: www.elsevier.com/locate/bios

Carbon nanotube electric immunoassay for the detection of swine influenza virus H1N1

Dongjin Lee[a], Yogesh Chander[b], Sagar M. Goyal[b], Tianhong Cui[a,*]

[a] Department of Mechanical Engineering, University of Minnesota, 111 Church St. S.E., Minneapolis, MN 55455, USA
[b] Department of Veterinary Population Medicine, University of Minnesota, 1333 Gortner Ave, Saint Paul, MN 55108, USA

ARTICLE INFO

Article history:
Received 6 October 2010
Received in revised form 20 January 2011
Accepted 20 January 2011
Available online 28 January 2011

Keywords:
Carbon nanotube
Swine influenza virus H1N1
Biosensor
Virus sensor
Immunoassay

ABSTRACT

A low-cost, label-free, ultra-sensitive electric immunoassay is developed for the detection of swine influenza virus (SIV) H1N1. The assay is based on the excellent electrical properties of single-walled carbon nanotubes (SWCNTs). Antibody–virus complexes influence the conductance of underlying SWCNT thin film, which has been constructed by facile layer-by-layer self-assembly. The basic steps of conventional immunoassay are performed followed by the electric characterization of immunochips at the last stage. The resistance of immunochips tends to increase upon surface adsorption of macromolecules such as poly-L-lysine, anti-SIV antibodies, and SIVs during the assay. The resistance shift after the binding of SIV with anti-SIV antibody is normalized with the resistances of bare devices. The sensor selectivity tests are performed with non-SIVs, showing the normalized resistance shift of 12% as a background. The detection limit of 180 $TCID_{50}$/ml of SIV is obtained suggesting a potential application of this assay as point-of-care detection or monitoring system. This facile CNT-based immunoassay also has the potential to be used as a sensing platform for lab-on-a-chip system.

1. Introduction

The novel H1N1 swine influenza virus (SIV) has spread worldwide resulting in a pandemic consisting of 135,000 cases and 816 deaths by mid-2009 (Khan et al., 2009). The SIV causes an acute respiratory disease and is transmissible to humans causing high fever, lethargy, nasal discharge, coughing, and dyspnea (Choi et al., 2002). The pandemic influenza A is transmitted from person to person by exposure to infected secretions. Conventional methods of virus diagnosis including virus isolation, polymerase chain reaction (PCR), and enzyme-linked immunosorbent assay (ELISA) require extensive sample handling, laboratory infrastructure, and long sample-to-result time (Lee et al., 1993). Although the reverse transcriptase-PCR demonstrated the lowest detection limit of less than 0.1 $TCID_{50}$/ml for SIV (Lekcharoensuk et al., 2006), it was offset by the need for sophisticated bench-top instrumentation, tedious and time-consuming sample preparation, and inclusion of trained personnel. Furthermore, the amount of sample available is often very small e.g., blood and cerebrospinal fluid from a neonate. Hence, it is desirable to develop a simple, sensitive, reliable and inexpensive antigen detection technique.

Immunosensors are analytical devices that yield sensitive, selective, and measurable signals in response to specific antigen–antibody interactions. They play the role of direct monitoring of molecular recognition event and consequently the diagnosis of pathogens. A variety of immunosensors has been developed using different transducers that exploit changes in mass (Vaughan et al., 2001), heat (Pizziconi and Page, 1997), electrochemical (Plekhanova et al., 2003; Sadik and Van Emon, 1996; Sklaal, 1997), or optical properties (Duendorfer and Kunz, 1998; Kubitschko et al., 1997; Marks et al., 2000). Of various transduction mechanisms, the electric detection of viruses (Dastagir et al., 2007; Mannoor et al., 2010; Nebling et al., 2003) has a potential to revolutionize traditional laboratory assays for pathogen detection, since it can be implemented easily overcoming disadvantages of the traditional assay. The portable personal devices including electrometer unit can be used to measure electrical signals from the assay. It is advantageous to point-of-care detection application in that other transduction mechanisms need the expensive and sophisticated instruments to measure output signal. For example, expensive quartz crystals and precise optical gears should be used in quartz crystal microbalance and surface plasmon resonance, respectively.

The carbon nanotubes (CNTs) are one of the most promising materials for the rapid detection of human and animal pathogens due to their excellent properties (Rica et al., 2008). The CNT-based biosensors have attracted much attention due to the availability of inexpensive off-the-shelf building blocks, miniaturized devices for small sample volumes and excellent transducing properties. In

* Corresponding author. Tel.: +1 612 626 1636; fax: +1 612 625 6069.
E-mail address: tcui@me.umn.edu (T. Cui).

0956-5663/$ – see front matter © 2011 Elsevier B.V. All rights reserved.
doi:10.1016/j.bios.2011.01.029

addition, CNTs enable a better biotic–abiotic interface due to their size similarity and the immobilized biomolecules preserve their bioactivities such as enzymatic reactions and recognition functions (Rica et al., 2008). The unique electrochemical transduction functions found previously (Lee and Cui, 2009b, 2010) sustain the application of CNTs to biosensing toward the label-free detection. Lastly, sensing platforms exploiting nanomaterials can be miniaturized to realize an autonomous one-shot sample-to-result bioassay via a sensing array incorporated into micro/nanofluidic systems.

Nanomaterials were widely used for the electrical detection of immuno-reaction. Label-free and real time detection of virus was done through silicon nanowire transistors (Patolsky et al., 2004). It showed discrete conductance change upon binding/unbinding of virus to the accepter molecules immobilized on nanowire. Furthermore, metal oxide nanowires were used to detect biomarker N-protein for severe acute respiratory syndrome virus using antibody mimic proteins resulting in sensitivity of sub-nanomolar concentration (Ishikawa et al., 2009). Hepatitis C virus RNA was electrically detected in the range of pico-molar concentration via SWCNT field effect transistors (Duendorfer and Kunz, 1998). Anti-hemagglutinin was detected through immune-reaction on the back-gate SWCNT transistor where hemagglutinin was immobilized. The detection limit of 5×10^{-8} mg/ml was found, which was three orders lower magnitude than the conventional ELISA technique. Influenza virus hemagglutinin could be a target molecule by immobilizing anti-hemagglutinin on the CNT FET surface (Takeda et al., 2007).

Herein, we report self-assembled CNTs random network thin film for the electrical detection of SIV H1N1. The resistance shifts upon virus binding were normalized with the resistance of bare devices, which extended the detection range with decreasing the channel length of CNT resisters. The CNTs networks were able to successfully detect as low as 180 $TCID_{50}$/ml of SIV using normalized resistance shift upon immunobinding of viruses. The sensor selectivity was shown against non-SIV viruses e.g., transmissible gastroenteritis virus (TGEV) and feline calicivirus (FCV). Based on combinative low-cost fabrication method of large-scale microfabrication and self-assembly, the immunochip is disposable after assay and designed as an on-site diagnostic tool to promptly control the epidemic viruses. Therefore, this facile CNT-based electric immunoassay has potential applications as a point-of-care test or a component for lab-on-a-chip system. Furthermore, the antibody-based assays can be utilized for developing portable assays for clinical diagnosis of SIV H1N1, combining with micro/nanofluidic systems.

2. Experiment

2.1. Materials and methods

Carbon nanotubes (90% of SWCNTs, 95% of CNTs, diameter: 1–2 nm, length: 5–30 μm, SSA: 300–380 m^2/g) used in this study were from Nanostructured and Amorphous Materials, Inc., Houston, TX. Pristine SWCNTs were functionalized as done previously to graft hydrophilic carboxylic groups for the stable dispersion to water (Lee and Cui, 2009b). As a result of chemical functionalization in concentrated acid, carboxylic groups were induced, which was evidenced by Fourier Transform Infrared spectroscopy demonstrating a strong peak at 1760 cm^{-1} (Lee and Cui, 2009a). Polyelectrolytes used for layer-by-layer assembly as a polycation and polyanion were poly(diallyldimethyammonium chloride, PDDA, M_w = 200–350k, Sigma–Aldrich) and poly(stylenesulfonate, PSS, M_w = 70k, Sigma–Aldrich), respectively. The concentration of PDDA and PSS used was 1.4 wt% and 0.3 wt%, respectively, with 0.5 M sodium chloride (NaCl) for better surface coverage. Poly-L-lysine (PLL, 0.1 wt%, Sigma–Aldrich) was used to immobilize the anti-SIV antibody physically on the surface of SWCNTs.

Stable interface of nanotubes with biomolecules is essential for successful detection of target biomolecules. Covalent conjugation of antibodies on carboxylated CNTs using cross linker carbodiimide such as 1-ethyl-3-(3-dimethylaminopropyl)carbodiimide (EDC) has been widely used. However, it requires special consideration on the wet chemistry such as choice of buffers and inter-protein conjugation. Furthermore, CNTs themselves have a strong affinity for biomolecules by means of electrostatic and hydrophobic interactions. It is not yet clear if covalent conjugation through carbodiimide cross linker is differentiated by electrostatic physical adsorption (Gao and Kyratzis, 2008). Therefore, we adopted a simple electrostatic interaction to immobilize antibody by employing PLL. The blocking buffer consisted of bovine serum albumin (BSA; Fraction V Solution 7.5%, Invitrogen Corp.) diluted to produce a 3% concentration in 1× PBS (KCl: 2.67 mM, KH_2PO_4: 1.47 mM, NaCl: 137.93 mM, $Na_2HPO_4 \cdot 7H_2O$: 8.06 mM).

Antiserum containing anti-SIV antibody was obtained from the National Veterinary Services Laboratory (NVSL, Ames, IA). The antibody titer determined by haemagglutinin inhibition (HI) assay was 1:1280. The antiserum was diluted 100-fold in 1× PBS to immobilize on SWCNTs. The SIV strain used in this study was obtained from the archives of the Minnesota Veterinary Diagnostic Laboratory (MVDL), University of Minnesota, Saint Paul, MN. The stock virus was propagated in Madin–Darby canine kidney (MDCK) cells. Cells infected with SIV were disrupted by three freeze–thaw cycles and cell debris was removed by centrifugation at 2000 × *g* for 10 min at 4 °C. The supernatant was collected, aliquoted (1 ml each in cryovials), and stored at −80 °C until the day of use. Appropriate dilutions of the stock virus were prepared in 3% BSA/PBS solution. Transmissible gastroenteritis virus (TGEV), a coronavirus of pigs, and feline calicivirus (FCV) used for determining specificity of the test were also from MVDL. The TGEV and FCV were grown in ST (swine testicular cells) and Crandell–Rees feline kidney (CRFK) cells, respectively.

2.2. Virus titration

The titration of FCV, TGEV, and SIV was done in CRFK, ST, and MDCK cells, respectively. Serial 10-fold dilutions of each virus were prepared in Eagle's Minimal Essential Medium (MEM). Virus dilutions were inoculated in monolayers of appropriate cells grown in 96-well microtiter plates using four wells per dilution. After the plates were incubated at 37 °C for 96 h, they were examined microscopically for virus-induced cytopathic effects (CPE). The highest dilution showing CPE was considered as the end point. Virus titers were calculated as previously described (Reed and Muench, 1938).

2.3. Fabrication of the immunochip

A standard 4 inch silicon (Si) wafer with thermally grown silicon dioxide (SiO_2 2 μm thick) was cleaned in a piranha solution (3:1 H_2SO_4:H_2O_2) at 120 °C for 15 min, rinsed thoroughly with a copious amount of deionized water (DIH_2O), and dried with a nitrogen (N_2) stream. Chromium (Cr, 300 Å) and gold (Au, 1000 Å) were electron-beam evaporated onto the Si/SiO_2 substrate and patterned for two electrodes using photolithography. Photoresist window was patterned to allow SWCNT to be assembled only on the conducting channel area. After the development of photoresist, oxygen (O_2) plasma was used to remove the residual photoresist completely on the opening window at a power of 100 W for 1 min with O_2 flow rate of 100 sccm as well as to make the surface hydrophilic, which is beneficial to the subsequent LbL assembly. The SWCNT multilayer thin film was assembled between microfabricated electrodes as a resistor. For thin film construction, two bi-layers of (PDDA/PSS)

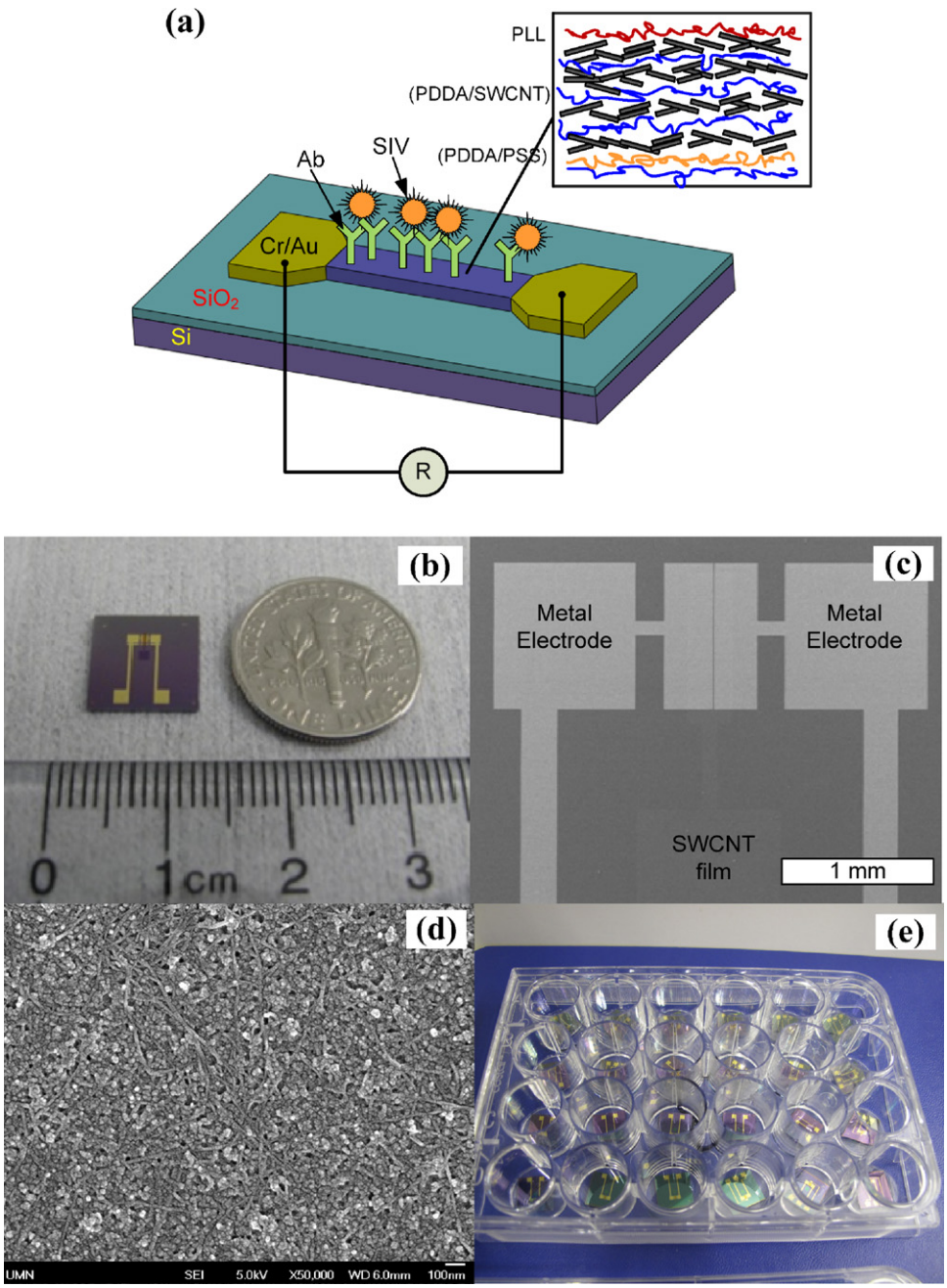

Fig. 1. The fabricated carbon nanotube thin film immunochips: (a) schematic of an individual immunochip with close-up hierarchy of SWCNT multilayer, (b) an optical image of the individual chip, SEM images of metal (Cr/Au) electrode pattern (c) and SWCNTs multilayer thin film between two electrodes (d), and (e) sorted immunochips in a 24-well plate for use in immunoassay. Conductance of SWCNT thin film changes due to antibody–virus complex.

were firstly self-assembled as a precursor layer on the patterned substrate for the charge enhancement followed by the assembly of $(PDDA/SWCNT)_5$ as an electrochemical transducing material. The dipping time used for polyelectrolytes and SWCNTs was 10 and 15 min, respectively. The silicon wafer was diced using wafer cutting system (Disco DAD 2H/6T).

2.4. Electric immunoassay

The resistance of the chips was measured using digital multimeter and recorded before the assay. Individual chips were sorted according to their channel length into 24-well tissue culture plates and the immunoassay was performed as follows. The chips were incubated in 0.3 ml of 0.1 wt% PLL for 1 h. The aqueous PLL was removed and 0.5 ml of distilled water (DW) was added. The plates were placed on a shaker for 2 min followed by the removal of DW. The rinsing process was repeated two more times followed by drying with nitrogen (N_2) stream. The resistance of the chips was measured and recorded. Next, 0.5 ml of 1:100 dilution of anti-SIV antibody in 1× PBS was added followed by incubation at 4 °C for 24 h. The immunochips were washed three times each in PBS and in DW followed by drying with N_2 stream and the measurement of resistance. To prevent nonspecific binding, 0.5 ml of 3% BSA/PBS was added. After incubation for 3 h at room temperature, 3% BSA/PBS was removed, chips washed in PBS and DW as described above, and resistance measured after drying. The devices were then incubated in 0.3 ml of various dilutions of SIV H1N1, TGEV, and FCV in 3% BSA/PBS and incubated for 1 h followed by rinsing, drying, and

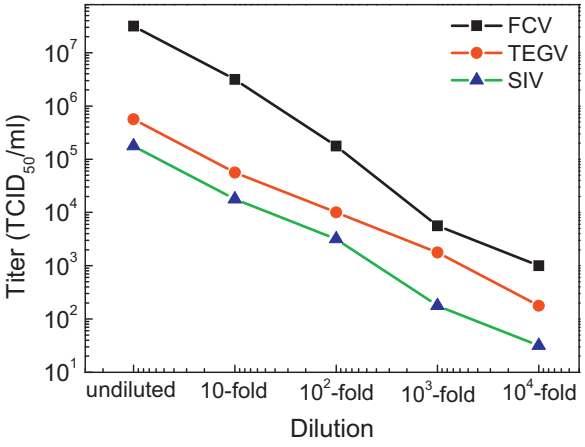

Fig. 2. Titers for serial 10-fold dilutions of FCV, TGEV, and SIV stocks used for the assay: the concentration exhibited a good linear relationship with the dilution.

resistance measurement. As a negative control, 3% BSA/PBS without any virus was used. The resistance shifts upon virus binding were normalized in three different ways: (a) with the resistances of bare chips (R_{chip}), (b) with the resistances after PLL assembly (R_{PLL}), and (c) with the resistances after anti-SIV antibody binding (R_{Ab}). The resistance shifts were normalized as follows:

$$\Delta R_x^* = \frac{R_{virus} - R_{Ab}}{R_x} \quad (1)$$

where x can be chip, PLL, or Ab indicating the resistance of bare devices, after PLL, and after antibody assembly, respectively.

3. Results and discussion

The SWCNT immunochip structure fabricated in this study is schematized in Fig. 1(a) including close-up hierarchy of thin film and antibody–virus complexes. It is a two-terminal device where the conductance of SWCNT thin film is subject to change due to the concentration of antibody–virus complexes. The diced individual immunochip is in size of 1 cm × 1 cm and SWCNT thin film was patterned so that it was confined to the conducting channel as shown in Fig. 1(b). The conducting channel dimension is 1 mm wide and 10, 20, and 50 μm long as shown in Fig. 1(c). The SEM image of SWCNT film in Fig. 1(d) demonstrates a random network of SWCNTs, which plays the role of transducer upon virus binding to its antibody. The immunochips were sorted into 24-well plates as shown in Fig. 1(e) in order to perform immunoassays.

Serial 10-fold dilutions of each virus showed the relationship with dilutions, as shown in Fig. 2. Undiluted FCV, TGEV, and SIV H1N1 samples had concentration of 3.16×10^7, 5.62×10^5, and 1.77×10^5 $TCID_{50}$/ml, respectively. A $TCID_{50}$ (50% tissue culture infective dose) means that the pathogen produces pathological changes in 50% of the cell cultures inoculated with the indicated virus amount.

I–V measurement was performed for the fabricated SWCNT resistor at the atmosphere, which demonstrated a linear relationship between current and voltage in both forward and backward biases in the range from −1 to 1 V indicating an ohmic contact between SWCNT film and metal electrode as well as among SWCNTs. The fabricated SWCNT resistors with variable lengths of 10, 20, and 50 μm possessing constant 1 mm width and 38 nm thickness were tested. Ten different devices from a same batch were tested and resistances were extracted by linear curve fitting, followed by plotting them as a function of channel length with the standard errors as error bars as shown in Fig. 3(a). The resistance was found to increase linearly with the conducting channel length

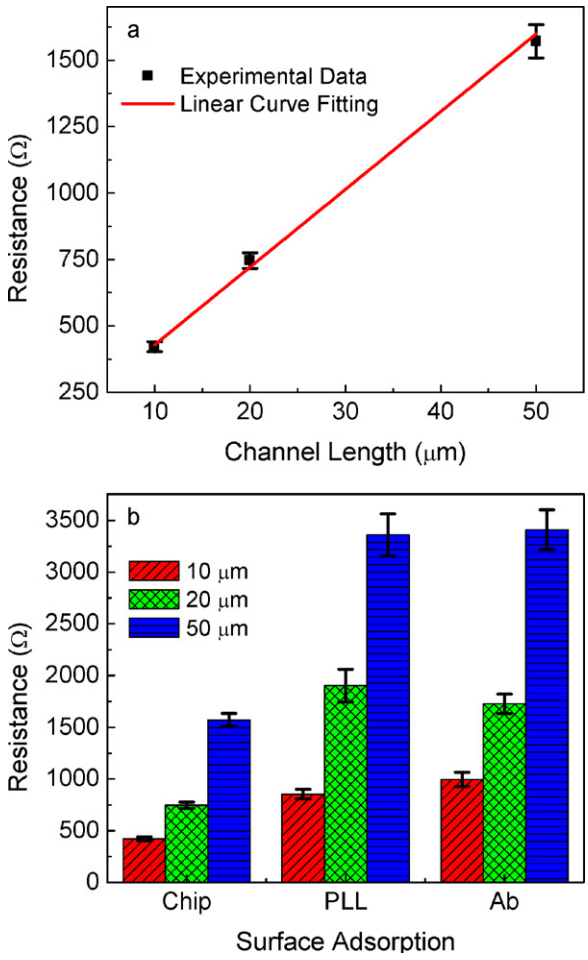

Fig. 3. The electrical characterization of SWCNT immunochips: (a) the resistance of layer-by-layer assembled SWCNT resistor with the width of 1 mm and thickness of 38 nm at variable channel lengths, and (b) the effect of surface adsorption on the resistance of chips with channel lengths of 10, 20, and 50 μm. Resistances significantly increase upon surface adsorption of PLL. Error bars indicate standard error from 10 devices in a batch.

demonstrating relationship of $R = 29.1 \times L + 140$, where R and L are in unit of Ω and μm, respectively.

The resistance measurement was also performed at each step of the immunoassay. The measured resistances of bare, PLL coated, and anti-SIV antibody assembled chips are shown with the standard error as error bars in Fig. 3(b). The resistance increases significantly upon PLL assembly presumably due to the drastically decreased charge carrier transfer caused by surface adsorption. However, it should be noted that antibody assembly on PLL layer does not influence resistance apparently as much as PLL does on SWCNTs. Once PLL is adsorbed on the sensitive CNT surface, there must be a significant electrostatic and/or structural change to induce observable resistance change. This suggests that the resistance changes after immunobinding of SIVs due to their charge carrier donating/accepting property and/or huge structure compared to SWCNT and antibody. The physical adsorption of viruses influences the electrical properties of SWCNT thin film which, in general, increases resistivity.

The resistance shifts after SIV binding at various virus dilutions are shown in Fig. 4. The resistance shift tends to increase with increasing concentration of SIV. The higher the SIV concentration, the more SIV adsorbs on the surface resulting in increased resistance of SWCNT film. Immunochips with 10 μm channel length exhibit a resolution down to 10^4-fold dilution, but the saturated resistance change at high concentrations from undiluted to 10^2-

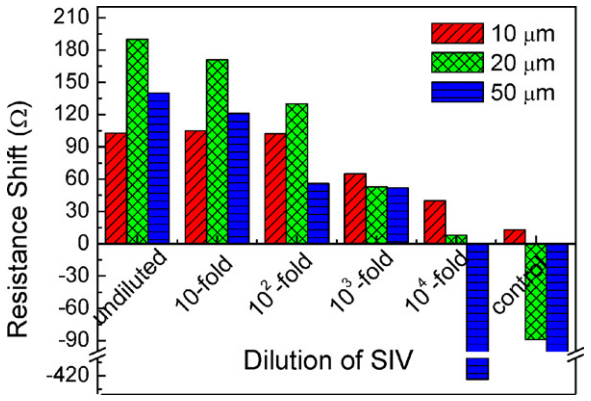

Fig. 4. Resistance shift upon immunobinding of SIV on channel lengths of 10, 20, and 50 μm: binding tends to increase with the concentration of SIVs. This suggests controllable detection range and detection limit in terms of sensing area.

fold dilution is observed. On the other hand, the plateau at high concentration is not observed in immunochips with 20 and 50 μm channel lengths. However, it is noted that those devices show a resolution at 10^3-fold dilution. The reason for the significant deviation at lower concentration and control immunochips with 20 and 50 μm channel lengths is that open binding sites in anti-SIV antibodies over the large area might be susceptible to other molecules present in a virus solution, causing unstable resistance shift. This indicates that the sensing area plays an important role in controlling the detection range and limit of detection. The larger sensing area can detect a higher concentration, yielding a lower resolution, which further suggests the use of nanoscale conducting gap or nanoscale individual materials could yield higher resolution. It is noticeable that the sensitivity of 30–40 Ω/decade is observed on each detection range irrespective of the sensing area.

The resistance shifts on virus binding ($R_{virus} - R_{Ab}$) on 10 μm channel length were normalized in order to address the variation in resistance of bare chips as depicted in Fig. 5. The average and standard error were extracted from 5 sets of immunoassay. The amount of virus bound corresponds to the resistance shift, and it is dependent on the amount of antibody as well. The immobilized antibody is proportional to effective binding area on PLL, ultimately on SWCNT film. For this reason, variation in amount of SWCNT, PLL, and antibody is resolved by normalization. Once the resistance shifts were normalized with the resistances of bare chips (R_{chip}), the

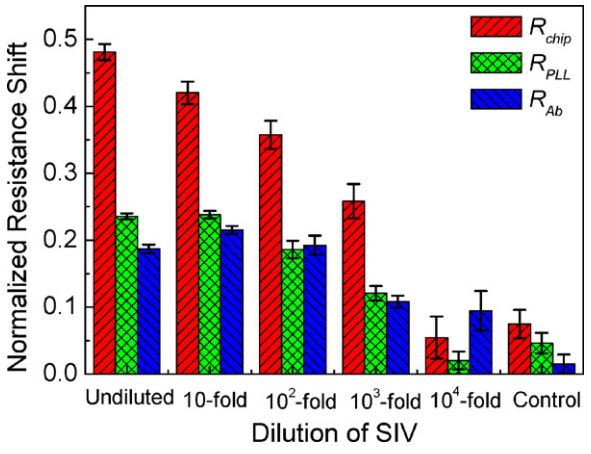

Fig. 5. The normalized resistance shift with the resistance of bare chips (R_{chip}), PLL coated (R_{PLL}), and anti-SIV antibody assembled chips (R_{Ab}) in 10 μm channel: the sensitivity increased significantly upon normalization with bare chips while the plateau is observed from undiluted to 10^2-fold dilution in the normalization with (R_{PLL}) and (R_{Ab}). The error bars indicate standard error from 5 sets of assays.

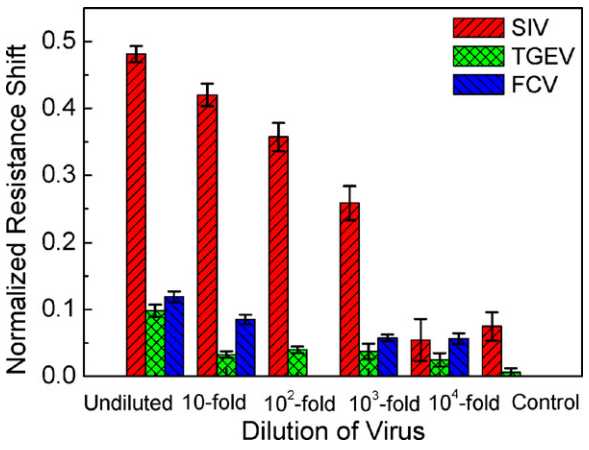

Fig. 6. Sensor selectivity tests of 10 μm channel immunochips against TGEV and FCV based on normalization with the resistance of bare chips (R_{chip}). The error bars indicate standard error from 5 sets of assays.

sensitivity is about 7.3%/decade on the range of undiluted sample to 10^3-fold dilutions. However, the sensitivities upon normalization with the resistances after PLL (R_{PLL}) and antibody adsorption (R_{Ab}) were almost the same, which is about 5.9%/decade on 10^1- to 10^3-fold dilutions. Moreover, the discernible signal was obtained on the saturated region, undiluted to 10^2-fold dilution when only resistance shift was considered in Fig. 4. Therefore, increased sensitivity and extended detection range could be obtained by employing appropriate normalization method.

The selectivity tests were conducted against TGEV and FCV using all 10 μm channel chips, and a typical result is shown in Fig. 6. All resistance shifts were normalized with the resistance of bare chips (R_{chip}) since it yielded the increased sensitivity in Fig. 5. The average and standard error here also were determined from 5 sets of immunoassay. The normalized resistance changes for FCV and TGEV were within 12% and 9% in all dilutions, while the normalized resistance shifts for SIV showed more than 25% on the range of undiluted to 10^3-fold dilution. The reason for a higher background signal for FCV than for TGEV assay might be a significant nonspecific binding of virus presumably due to 2 orders higher concentration of the undiluted virus stock as identified in Fig. 2. The control and 10^4-fold dilution of SIV revealed background signal of less than 10%. As a result of selectivity test, the detection of SIV is selective down to 10^3-fold dilution (1.77×10^2 $TCID_{50}$/ml). The range of influenza viral particles 10^3–10^5 $TCID_{50}$/ml has been found in the infected swine nasal samples (Reichmuth et al., 2008). Therefore, the electronic detection of SIV, which revealed a detection limit of about 180 $TCID_{50}$/ml, has the potential for rapid on-site diagnosis and/or monitoring. These results are comparable to detection limit of 610 $TCID_{50}$/ml SIV using microchip-based electrophoretic immunoassays (Reichmuth et al., 2008).

4. Conclusions

The SWCNTs network can be used as a low-cost, label-free, ultra-sensitive, and electric detection of SIVs. The electrical resistance increased upon surface adsorption of macromolecules such as PLL. Furthermore, the immunobinding of SIV on the sensor surface notably changed the resistance of SWCNTs thin film. The resistance shifts upon virus binding were normalized with the resistance of bare chips, which enhanced the sensitivity and removed the plateau at high concentration. The detection limit of SWCNT network for SIVs has been obtained as 10^3-fold dilution from multiple tests with about 10% background signal. The selectivity test also indicated that 10^3-fold dilution of SIV could be detected against FCV

and TGEV. The detection limit of 10^3-fold dilution of SIV amounts to 180 $TCID_{50}$/ml. The antibody-based assays can be utilized as a portable device for the clinical diagnosis of SIV H1N1. The facile electronic detection of viruses via CNTs resistors can be used as the point-of-care detection and the component of lab-on-a-chip. Furthermore, it can be extended to other elegant analytical assays once it is combined with micro/nanofluidic systems.

Acknowledgments

The authors acknowledge the DARPA M/NEMS Science and Technology Fundamentals Research Program for funding support through the Micro/Nano Fluidics Fundamentals Focus (MF3) Center. A part of this work was conducted at the Nanofabrication Center and Characterization Facility at the University of Minnesota, which are partially supported by NSF through the NNIN program.

Appendix A. Supplementary data

Supplementary data associated with this article can be found, in the online version, at doi:10.1016/j.bios.2011.01.029.

References

Choi, Y.K., Goyal, S.M., Kang, S.W., Farnham, M.W., Joo, H.S., 2002. J. Virol. Methods 102 (1–2), 53–59.
Dastagir, T., Forzani, E.S., Zhang, R., Amlani, I., Nagahara, L.A., Tsui, R., Tao, N., 2007. Analyst 132 (8), 738–740.
Duendorfer, J., Kunz, R.E., 1998. Appl. Opt. 37 (10), 1890–1894.
Gao, Y., Kyratzis, I., 2008. Bioconjug. Chem. 19 (10), 1945–1950.
Ishikawa, F.N., Chang, H.-K., Curreli, M., Liao, H.-I., Olson, C.A., Chen, P.-C., Zhang, R., Roberts, R.W., Sun, R., Cote, R.J., Thompson, M.E., Zhou, C., 2009. ACS Nano 3 (5), 1219–1224.
Khan, S.I., Akbar, S.M.F., Hossain, S.T., Mahtab, M.A., 2009. Rural Remote Health 9 (1262), 1–4.
Kubitschko, S., Spinke, J., Brukner, T., Pohl, S., Oranth, N., 1997. Anal. Biochem. 253 (1), 112–122.
Lee, B.W., Bey, R.F., Baarsch, M.J., Simonson, R.R., 1993. J. Vet. Diagn. Invest. 5 (4), 510–515.
Lee, D., Cui, T., 2009a. IEEE Sens. J. 9 (4), 449–456.
Lee, D., Cui, T., 2009b. J. Vac. Sci. Technol. B 27, 842–848.
Lee, D., Cui, T., 2010. Biosens. Bioelectron. 25, 2259–2264.
Lekcharoensuk, P., Lager, K.M., Vemulapalli, R., Woodruff, M., Vincent, A.L., Richt, J.A., 2006. Emerg. Infect. Dis. 12 (5), 787–794.
Mannoor, M.S., Zhang, S., Link, A.J., McAlpine, M.C., 2010. PNAS 107, 19207–19212.
Marks, R., Margalit, A., Bychenko, A., Bassis, E., Porat, N., Dagan, R., 2000. Appl. Biochem. Biotechnol. 89 (2), 117–126.
Nebling, E., Grunwald, T., Albers, J., Schafer, P., Hintsche, R., 2003. Anal. Chem. 76 (3), 689–696.
Patolsky, F., Zheng, G., Hayden, O., Lakadamyali, M., Zhuang, X., Lieber, C.M., 2004. PNAS 101 (39), 14017–14022.
Pizziconi, V.B., Page, D.L., 1997. Biosens. Bioelectron. 12 (4), 287–299.
Plekhanova, Y.V., Reshetilov, A.N., Yazynina, E.V., Zherdev, A.V., Dzantiev, B.B., 2003. Biosens. Bioelectron. 19 (2), 109–114.
Reed, L.J., Muench, L.H., 1938. Am. J. Hyg. 27 (3), 493–497.
Reichmuth, D.S., Wang, S.K., Barrett, L.M., Throckmorton, D.J., Einfeld, W., Singh, A.K., 2008. Lab Chip 8 (8), 1319–1324.
Rica, R.D.L., Mendoza, E., Lechuga, L.M., Matsui, H., 2008. Angew. Chem. Int. Ed. 47 (50), 9752–9755.
Sadik, O.A., Van Emon, J.M., 1996. Biosens. Bioelectron. 11 (8), i–x.
Sklaal, P., 1997. Electroanalysis 9 (10), 737–745.
Takeda, S., Ozaki, H., Hattori, S., Ishii, A., Kida, H., Mukasa, K., 2007. J. Nanosci. Nanotechnol. 7, 752–756.
Vaughan, R.D., O'Sullivan, C.K., Guilbault, G.G., 2001. Enzyme Microb. Technol. 29 (10), 635–638.